CEA/SACLAY
DSM

DAPNIA/SPHN-99-13   03/1999

Pulse height defect in the passivated ion-implanted Si detectors of the INDRA array

G. Tabacaru, B. Borderie, A. Ouatizerga, M. Parlog, M.F. Rivet, G. Auger, Ch.O. Bacri,
F. Bocage, R. Bougault, R. Brou, Ph. Buchet, J.L. Charvet, A. Chbihi, J. Colin, D. Cussol,
R. Dayras, A. Demeyer, D. Doré, D. Durand, P. Ecomard, J.D. Frankland, E. Galichet,
E. Genouin-Duhamel, E. Gerlic, D. Guinet, P. Lautesse, J.L. Laville, J.F. Lecolley,
A. Le Fèvre, T. Lefort, R. Legrain, N. Le Neindre, O. Lopez, M. Louvel, L. Nalpas,
A.D. Nguyen, J. Péter, E. Plagnol, E. Rosato, F. Saint-Laurent, S. Salou, M. Squalli,
J.C. Steckmeyer, M. Stern, B. Tamain, L. Tassan-Got, O. Tirel, E. Vient, C. Volant
and J.P. Wieleczko

DAPNIA

Couverture Sylvie Cabrit et Marc Sauvage

Pulse height defect in the passivated ion-implanted Si detectors of the INDRA array

G. Tăbăcaru [a,b], B. Borderie [a], A. Ouatizerga [a], M. Pârlog [b],
M.F. Rivet [a], G. Auger [c], Ch.O. Bacri [a], F. Bocage [d],
R. Bougault [d], R. Brou [d], Ph. Buchet [e], J.L. Charvet [e],
A. Chbihi [c], J. Colin [d], D. Cussol [d], R. Dayras [e], A. Demeyer [f],
D. Doré [e], D. Durand [d], P. Ecomard [c], J.D. Frankland [a],
E. Galichet [f], E. Genouin-Duhamel [d], E. Gerlic [f], D. Guinet [f],
P. Lautesse [f], J.L. Laville [c], J.F. Lecolley [d], A. Le Fèvre [c],
T. Lefort [d], R. Legrain [e], N. Le Neindre [d], O. Lopez [d],
M. Louvel [d], L. Nalpas [e], A. D. Nguyen [d], J. Péter [d],
E. Plagnol [a], E. Rosato [g], F. Saint-Laurent [c,1], S. Salou [c],
M. Squalli [a], J.C. Steckmeyer [d], M. Stern [f], B. Tamain [d],
L. Tassan-Got [a], O. Tirel [c], E. Vient [d],
C. Volant [e] and J.P. Wieleczko [c]

[a] *Institut de Physique Nucléaire, IN2P3-CNRS, F-91406 Orsay Cedex, France*

[b] *National Institute for Physics and Nuclear Engineering, RO-76900 Bucharest-Măgurele, Romania*

[c] *GANIL, CEA, IN2P3-CNRS, B.P.5027, F-14076 Caen Cedex 5, France*

[d] *LPC, IN2P3-CNRS, ISMRA et Université, F-14050 Caen Cedex, France*

[e] *DAPNIA/SPhN, CEA/Saclay, F-91191 Gif sur Yvette Cedex, France*

[f] *Institut de Physique Nucléaire, IN2P3-CNRS et Université, F-69622 Villeurbanne Cedex, France*

[g] *Dipartimento di Scienze Fisiche, Univ. Federico II, I80126 Napoli, Italy*

Abstract

The pulse height defect (PHD) of ^{36}Ar, ^{58}Ni, ^{129}Xe, ^{181}Ta and ^{197}Au ions in the 180 passivated ion-implanted silicon detectors of the INDRA array has been measured. The detectors faced the target with the low electric field side. The charge encoding ensured a low ballistic deficit. Detectors with the same nominal characteristics and electric field strength show a PHD dependence on the individual silicon wafer. They are classified and calibrated by using an empirical parametrization which relates

the PHD to the total energy through a Z-depending power law. A PHD analytical formula, based on a simple recombination model, is also proposed. It considers a realistic charge density variation with the position coordinate on the ion path. This new formula is successfully confronted to some experimental data.

1 Introduction

In the last decade surface-barrier silicon detectors have been frequently replaced by passivated ion-implanted silicon detectors. This substitution is most effective in heavy ion collision experiments with, in particular, the advent of multidetectors like INDRA, covering large surfaces and/or large solid angles and for which the photolithography of the planar process is very convenient. Therefore information on the energy response of these new detectors to heavy ions is of great interest [1], most of the available data referring to surface-barrier detectors. INDRA is a 4π axially symmetrical array for the detection of light and heavy nuclear reaction products [2,3]. It has a high granularity and a shell structure, consisting of several detection layers, including a silicon one. Reliable energy calibration procedures for each of the detection layers are necessary. For the silicon shell, the method considers, as usual, the electronic non-linearity and, when heavy ions are detected, a pulse height defect (PHD). Indeed the pulse height produced by a heavy ion ($Z{\geq}10$) in a silicon detector is smaller than that of a light ion depositing the same energy in the detector. This effect is referred to as PHD and must be taken into account in calibration procedures. For this purpose, a study of the heavy ion PHD in the 180 passivated ion-implanted silicon detectors of INDRA was performed and empirical parametrizations for different detector groups were derived in the framework of the Moulton et al. procedure [4]. Results are also compared to an analytical formula relating the PHD to the mass, charge and incident energy, developed here in the formalism of a simple recombination model without diffusion, and finally to other PHD available calculations [5,6].

Section 2 briefly describes the geometry and particularities of the silicon detectors and related details of the associated electronics. The energy calibration of the silicon detectors for light charged particles (LCP) and light fragments (LF, $Z{\leq}10$) is directly obtained by a classical recipe and detailed in section 3. For heavy fragments (HF), the PHD data are carried out by measuring the energy of 6 – 10 AMeV heavy ion beams delivered by the first GANIL cyclotron and elastically scattered by a gold target. The measured PHD val-

---

[1] present address: CEA, DRFC/STEP, CE Cadarache, F-13108 Saint Paul lez Durance Cedex, France

Pre-amplifiers

Photomultipliers

4 Cesium Iodide
(5-14 cm)

4 Silicon detectors
(300μm)

cathode **Anode**

1 Ionisation Chamber
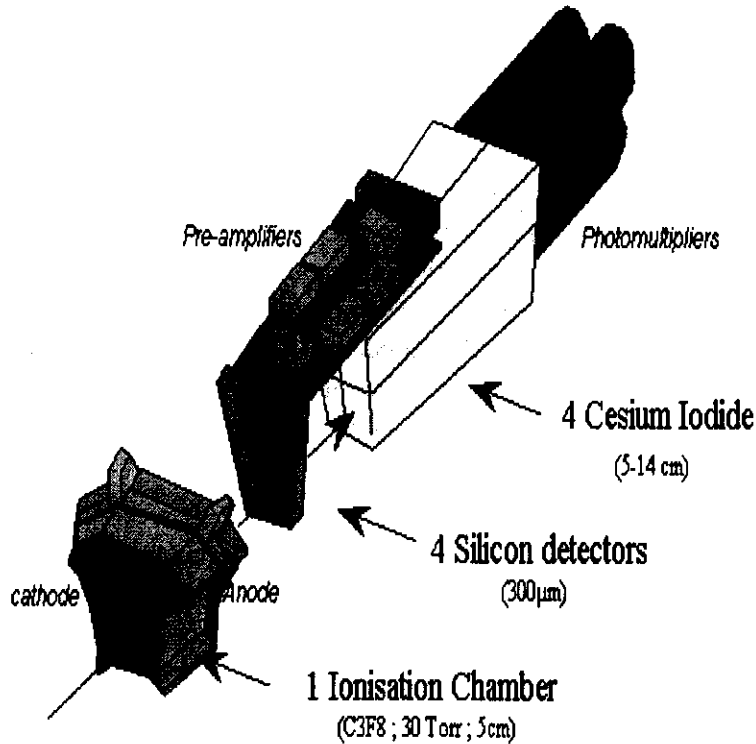(C3F8 ; 30 Torr ; 5cm)

Fig. 1. A detection cell of INDRA is composed of three layers: 1 ionisation chamber, 4 silicon detectors designed on the same wafer and their preamplifiers and 4 CsI(Tl) scintillators and their photomultipliers.

ues are parametrized with an empirical formula described in section 4. The predictions of several calculations which quantify the PHD of heavy ions in solid state detectors are confronted to our experimental results in section 5. Our findings are summarized in section 6.

2 The silicon detectors and related details

2.1 Geometry

The 336 independent cells of INDRA are placed on 17 rings ($2° < \theta < 176°$) [2]. Forward cells (rings: 2 – 9, covering $3° < \theta < 45°$) have a "sandwich" structure of three layers: gas ionisation chamber (IC), 300 μm thick silicon detector (Si) and thallium activated cesium iodide scintillator (CsI(Tl)). Fig. 1 shows a detection cell with three layers. The polar angular opening of the silicon detectors lies between 1.5° (ring 2) and 10° (ring 9).

The passivated ion-implanted silicon detectors were made by Eurisys Mesures [7] by means of the planar process. High resistivity silicon of about 10 KΩcm was used. The photolithography of the process [8] provides the possibility of conceiving a mosaic with several detectors on the same wafer and extending the sensitive area up to its edges. Three or four pads from two adjacent rings (2 − 3, 4 − 5, 6 − 7, 8 − 9) were designed on the same silicon wafer (48 wafers in all), minimizing in this way the dead zones resulting from the mechanical supports. There are 180 Si detectors: 12 modules on ring 2 and 24 on each of the rings 3 − 9.

In order to avoid cross talk effects due to the capacitive coupling between the IC anode and the Si detectors placed just behind, the side of these detectors facing the IC must be grounded. As the pads are necessarily designed on the p+ side, the ground side must be the n+ one. Consequently, the particles enter the detectors by the low electric field side. The detectors were fully depleted and even over-biased [2] at the operating voltage V. The electric field strength F inside the detector varies linearly with the depth x from the n+ entrance side [9]:

$$F = \frac{2 \cdot V_s}{d^2} \cdot x + \frac{V - V_s}{d} \tag{1}$$

where d is the depletion depth and depends on the permitivity $\varepsilon = 11.8$, the resistivity ρ, the electron mobility $\mu \approx 1400 \text{ cm}^2\text{V}^{-1}\text{s}^{-1}$, and the depletion bias V through the relation $d = (2 \cdot \varepsilon \cdot \rho \cdot \mu \cdot V)^{1/2}$. When d is equal to the detector thickness, the detector is fully depleted and the corresponding bias is V_s. By entering the low field side, a particle slowing down in the detector loses more and more energy per depth unit, because its stopping power increases with x, but it moves in a higher and higher electric field. This configuration has therefore a compensatory effect concerning the carrier recombination process. On the other hand, for a fragment which stops near the entrance side, the electric field averaged over its range is smaller than it would had been by entering the high field side. Table 1 gives the resistivities, the depletion and operating biases (one power supply per silicon wafer) which are the same for the detectors belonging to two adjacent rings, as well as the minimum and the maximum electric field. The reverse orientation of INDRA's silicon detectors, together with their high resistivity are particularities to be kept in mind when the present PHD results are compared to other available data.

4

Table 1

Resistivity ρ, depletion bias V_s (from [7]), operation bias V, minimum electric field strength F_{min} and maximum electric field strength F_{max} for the silicon detectors of INDRA.

Rings	$\rho[K\Omega cm]$	$V_s[V]$	$V[V]$	$F_{min}[V/cm]$	$F_{max}[V/cm]$
2 – 3	9.0	40	80	1333.3	4000.0
4 – 5	9.0	40	50	333.3	3000.0
6 – 7	14.4	25	30	166.6	1833.3
8 – 9	9.0	40	50	333.3	3000.0

2.3 Electronics and stability control

The electronics of INDRA and the data acquisition system are described in details elsewhere [2,3]. Each Si detector is connected to a charge preamplifier, housed in the proximity of the detector. Its energy sensitivity is 2 mV/MeV with a maximum output amplitude of 10 V. The signal is shaped in a low noise (< 100 KeV FWHM) amplifier of weak gain, especially developed [3,10]. It consists of 1.5 μs CR-RLC filters followed by a clamp circuit and it gives a negative unipolar signal with a width (3.5 μs) which is practically independent of amplitude. The analog to digital conversion is achieved by double charge encoding: two integrators with gain ratios 1:16 and two multiplexed 12 bit converters, which allows to cover the energy range 1–5000 MeV. In our hyperpure, high resistivity silicon detectors, the carrier life-time is about 10 ms long. The ballistic deficit of the INDRA electronics using charge to digital converters (QDCs) is ten times smaller than in the case of chains based on spectroscopy amplifiers and peak sensing ADCs [3].

The linearity of the electronic chains was checked by means of 6 precision pulse generators, each one having 8 channels. The preamplifiers attached to the pads of a silicon wafer share the same generator signal. The nonlinearities did not exceed 10^{-4} on the whole dynamic range. Using the fact that the beam was sent to another cave for 10 % of the time, the stability of the electronic chain was permanently controlled during data acquisition by sending pulser signals during this time. It was thus found that the pedestals of the QDC's fluctuate slightly with time. These fluctuations are monitored by the channel position x_G of the pulser signal of fixed amplitude V_G. This allows to completely correct the physical spectra off-line, event by event. There is a number of electronic chains for which a supplementary contribution to x_G was put in evidence by software. It comes from an off-set of ≈ 1 mV introduced by one of the pulse generators. It can be corrected only on average, as we shall see in the next section.

3 Energy calibration for light charged products

3.1 General procedure

The energy calibration proceeds through three stages which are accomplished in each experimental campaign:

i) a voltage calibration of the electronic chain associated to each silicon detector by varying the amplitude of the pulse generator; it provides an *amplitude-channel* correspondence as well as the chain linearity;

ii) the conversion of the pulse generator amplitude [Volt] into energy unit [MeV] by means of the two alpha peaks from a thoron (^{212}Bi/^{212}Po) source; this *energy-voltage* correspondence furnishes the factor MeV-Volt, which allows finally to get the *energy-channel* correspondence of interest;

iii) the determination of the heavy ion PHD in the silicon detectors from elastic scattering data.

The stages i) and ii) are presented in this section, and the stage iii) in the next section.

The slight non-linearity of the electronic chain associated to a given Si detector (preamplifier, amplifier and QDC) is quantified in a parabolic dependence of the pulser voltage amplitude V versus the corresponding channel x of the QDC:

$$V(x) = a_0 + a_1 \cdot x + a_2 \cdot x^2 \qquad (2)$$

The reference coefficients a_0, a_1, a_2 are related to meaningful quantities: a_0 to the QDC pedestal $x_{0_{ref}}$ ($V = 0$), a_1 to the gain and a_2 to the slight non-linearity ($a_2/a_1 \approx 10^{-4}$) of the chain. It was found that the coefficients a_1 and a_2 are very stable in time for all the chains, while the free term a_0 shows small fluctuations for part of the chains, mainly due to the fluctuations of the QDC pedestals. We remind that, in addition, one of the pulser has introduced an off-set of ≈ 1 mV, which also contributes to the a_0 value, then called a_{0_V}. For the reference pulser signal amplitude V_G, equation (2) reads:

$$V_G(x_G) = a_{0_V} + a_1 \cdot x_G + a_2 \cdot x_G^2 \qquad (3)$$

For each chain two peaks induced at channels x_1, x_2 by α particles of energies $E_1 = 5.55$ MeV and $E_2 = 8.41$ MeV are used. These α particles are provided by the thoron source and they reach the Si detector after passing through the first layer (IC) of the "sandwich" detection cell. The channels x_i, i=1,2 correspond to the centroids of the peaks and the energy loss in the source and

6

in the mylar windows of the empty IC are taken into account [11]. One may get the correspondence *energy-channel* via the correspondence *voltage-channel* (2)

$$E(x) = f \cdot V(x), \qquad (4)$$

where f is the unique conversion factor MeV-Volt of interest, the same for both "high" and "low gain" cases. The equation (4) is transcribed for the two alpha peak energies as follows:

$$E_i(x_i) = f \cdot (a_{0_E} + a_1 \cdot x_i + a_2 \cdot x_i^2), \qquad i = 1, 2 \qquad (5)$$

The equations (5) provide the factor "f" MeV-Volt and the free term a_{0_E} connected to the pedestal fluctuations only. By averaging the free term a_{0_E} over all the "α source" calibration runs and by means of equations (3) and (5), an approximate correction for the pulser off-set $\delta V = a_{0_V} - \langle a_{0_E} \rangle$ is calculated for each event, with a value of about 1 mV, if any. Finally, the energy E corresponding to the channel x, for one event belonging to a "physics" run, is:

$$E(x) = f \cdot (a_{0_V} - \delta V + a_1 \cdot x + a_2 \cdot x^2) \qquad (6)$$

The quality of the calibration was checked by means of light charged products ($Z \leq 4$) elastically scattered on C and Ta targets, which were mainly devoted to the energy calibration of the scintillators [2]. The energy of scattered particles entering the silicon detectors was calculated as shown in the following sub-section. The precision of the calibration is of about 2% over the whole range of the experimental spectra, except in the very low energy region (≤ 4 MeV), where it becomes a little bit worse, about 3-4%.

3.2 Estimate of the deposited energy

The beam energy is obtained from the magnetic rigidity of the analysing magnet, the "alpha" spectrometer of GANIL. The relative uncertainty is better than 10^{-3}. The elastically scattered ions enter the silicon detectors after passing through the IC which is either empty or filled with C_3F_8 gas. The energy deposited in the active region of a silicon detector is determined by Monte Carlo simulations starting from the beam energy, as follows. The target thickness (of a few hundreds of $\mu g/cm^2$), is divided into slices of 10 $\mu g/cm^2$ in which the scattering center may be eventually located. The energy loss in the target before scattering is calculated by means of stopping power tables of Hubert et al [11]. The energy lost afterwards by the scattered ion in the target and in the IC mylar windows is calculated with the same tables [11], while in C_3F_8

gas, an equivalent formula extracted from experimental measurements [12] is used. For our passivated ion-implanted silicon detectors, the energy lost in the entrance window (of about 1500Å) is neglected. The scattering polar angle θ is incremented, in steps of 1 degree from θ_{min} up to θ_{max}, in order to cover the angular opening of the detector $\Delta\theta = \theta_{max} - \theta_{min}$. The energy, weighted by the Rutherford cross section $d\sigma/d\Omega$ is averaged over the opening polar angle of the detector.

$$\langle E \rangle = \frac{\int_0^{2\pi} \int_{\theta_{min}}^{\theta_{max}} E(\theta) \frac{d\sigma}{d\Omega} d\Omega}{\int_0^{2\pi} \int_{\theta_{min}}^{\theta_{max}} \frac{d\sigma}{d\Omega} d\Omega} \tag{7}$$

This is the *true* energy attached to the centroid channel of the elastic peak in the experimental spectrum.

4 Pulse height defect and energy calibration for heavy fragments

4.1 Pulse height defect in INDRA silicon detectors

If compared to the response to alpha particles, the energy response of silicon detectors to heavy ions is attenuated and shows non-linearities which are charge, mass and energy dependent. This attenuation of the output signal is known as energy defect or pulse height defect (PHD). In fact, the PHD is the difference between the true energy of the heavy ion and that of an α particle required to produce the same pulse height in the detector: PHD = E_{true} - E_{alpha}. The PHD may reach up to several tens per cent of the *true* energy, requiring thus special calibration techniques for determination of the true energy of the heavy ion [4–6].

There are several processes which lead to the attenuation of the output signal induced by heavy ions:

i) the energy loss in the entrance window;

ii) the recombination process, which becomes important when high density carriers are produced by strongly ionizing particles;

iii) the nuclear stoppping, which is no more negligible under 1 AMeV, i.e. at the end of the ion range;

iv) the ballistic deficit: the electric field strength is diminished by the space charge of the local plasma; consequently, the collection velocity is reduced and the rise time of the output signal increases.

The quality of the passivated ion-implanted silicon detectors (long carrier lifetime of about 10 ms, extremely thin dead zone of about 1500 Å) and the

8

electronics (charge encoding) of INDRA reduces the effects i), ii) and iv) and consequently the PHD, which is therefore mainly due to effects ii) and iii).

The PHD values also depend on the silicon resistivity and on the strength of the electric field inside the detector. We recall that the high resistivity Si detectors of INDRA face the target by their low field side (see Table 1). The measurements showed that for nuclei which stop in the Si detectors, the PHD values remain consistent with zero for light charged products ($Z \leq 10$). For heavy fragments, these values are significant and they increase with the atomic number of the fragment.

The PHD value ΔE of several heavy ions at low energy, stopped in the Si detectors, was determined from elastic scattering data of Ar, Ni, Xe and Ta by a Au target. With the Ta beam, PHD values from Au recoil were also measured. The beam energies were the following:

^{36}Ar at 8.06 AMeV and 9.04 AMeV
^{58}Ni at 9.08 AMeV and 9.73 AMeV
^{129}Xe at 7.65 AMeV
^{181}Ta at 6.02 AMeV

The point concerning the Ni ion was repeated in several experimental campaigns between 1993 and 1997. The results of the different campaigns are fully compatible. According to the kinematics, the energy E of a scattered projectile is a function of the angle θ, the same for all detectors of one ring of INDRA. The mean energies deposited in the silicon detectors, given by eq. (7), are listed in Table 2. For a given heavy ion we dispose of one or at most two energies per ring for the Si layer, corresponding to the two possible states of the IC layer: with gas inside (g) or empty (ng). This is the reason why the energy dependence of the PHD can not be analyzed for an individual module, but in the framework of a comparative study of the Si detectors placed on different rings. As written in table 1, the detectors belonging to one ring have the same global characteristics (resistivity and operating bias). However, the corresponding individual PHD values for these detectors can differ by more than a factor of two. For this reason, an approach of the PHD analysis by means of Kaufman [5] or Ogihara [6] methods, which contain as parameters the resistivity, or resistivity and field strength, respectively, was possible only for PHD values averaged over rings. This is not convenient because, for the energy calibration, the PHD parametrization has to be more precise. Fig. 2 shows the Ta PHD values for the detectors of rings number 2 and 3. As one may see, the individual values in Fig. 2 are rather different but they cluster however in two groups. The histogram in the top box represents the projection on the abscissa and it illustrates the two groups I and II in which the detectors of rings 2 and 3 have been shared. The same procedure was used to define groups for other double rings and finally 9 groups have been constituted.

Table 2

True energies in [MeV] deposited in Si by the Ni (9.73 AMeV), Xe, Ta and Au elastically scattered ions. Here "g" and "ng" refer to the two states of the IC: with gas and without gas, respectively.

Ring	Ni g	Ni ng	Xe ng	Ta g	Ta ng	Au g
2	502.90	544.20	922.96	820.20	992.00	
3	501.90	543.30	919.49	814.70	986.60	
4	499.90	541.40	911.91	802.90	975.10	
5	496.40	537.90	898.32	781.60	954.30	
6	489.20	531.00	871.87	740.20	913.90	
7	476.10	518.40	823.74	665.60	841.00	616.20
8	474.00	499.50	815.90	628.80		573.90
9			719.44	482.00		410.10

Groups I, III, V and VII correspond to the lowest PHD.

4.2 PHD parametrization

The PHD data have been treated in the framework of Moulton recipe [4], which relates the PHD value ΔE to the fragment energy E by a simple power law:

$$\Delta E = 10^{b(Z)} \cdot E^{a(Z)} \tag{8}$$

The general power index $a(Z)$ and the individual one $b(Z)$ are, as recommended by [4]:

$$a(Z) = 0.0223 * (Z^2/10^3) + 0.5682 \tag{9}$$

$$b(Z) = p_2 * (10^2/Z) + p_1 \tag{10}$$

Here, p_2 and p_1 are coefficients to be determined. In fact, equation (8) splits the PHD value ΔE of an impinging ion of atomic number Z and energy E in two terms: $E^{a(Z)}$ related to the energy and $10^{b(Z)}$ related to the individual detector properties. The dependence (9) of the energy power index a(Z) was checked and found to be correct within 2% for the detectors of ring number 2: the test was done by means of Xe beams of 7.65 AMeV and 25.0 AMeV elastically scattered by a gold target.
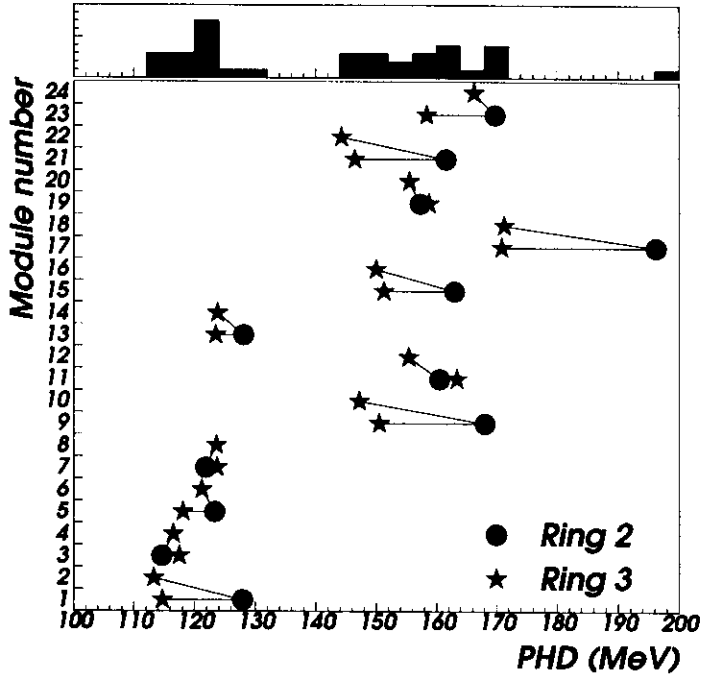
Fig. 2. Pulse height defect values for Ta (Z=73) in the silicon detectors of rings number 2 and 3 of INDRA. The projection on the abscissa is plotted in the top box. Lines connect the modules on the same wafer.

The quantity:

$$b(Z) = \log(\Delta E / E^{a(Z)}) \tag{11}$$

in the case of Ta ion (Z = 73) was chosen to classify the Si detectors. The advantage is that the detectors belonging to two adjacent rings and sharing common Si wafers can be analyzed and classified at the same time, in spite of the fact that the polar angles θ, and therefore the energies for two adjacent rings are different. Based on b(Z=73) every two adjacent rings were divided in two groups of detectors, except the rings 8 – 9 which show three groups. As expected, the individual detectors built on the same wafer always belong to the same group (see Fig. 2 for illustration). It was also observed that the widths of elastic spectra were correlated to PHD values: large widths correspond to large PHDs. Therefore, the fact that different wafers, having the same resistivity and operating bias, present various PHD values can be understood in terms of different resistivity variations in the detector bulk [13–15]. Indeed the manufacturer only gives average values for the characteristics of detectors. The nine groups of detectors are listed in Table 3.

11

Table 3

The nine groups of silicon detectors of INDRA classified under the individual power index $b(Z=73)$; (see the text for explanations). The last two columns give the values of the two parameters of eq. (10) for this work as well as for ref [1] and [4]

Group	Rings	Modules	p_2	p_1
I	2-3	1-8 13-14	-0.604	0.949
II	2-3	9-12 15-24	-0.530	0.969
III	4-5	1-16 23-24	-0.377	0.729
IV	4-5	17-22	-0.322	0.756
V	6-7	1-8 21-24	-0.290	0.661
VI	6-7	9-20	-0.262	0.705
VII	8-9	3-6	-0.500	0.790
VIII	8-9	9-14 17-20	-0.280	0.839
IX	8-9	1-2 7-8 15-16 21-24	-0.243	0.819
			-0.85 [1]	1.28 [1]
			-0.1425 [4]	0.0825 [4]

For each group of detectors, we have determined the experimental values of $b(Z)$, averaged over the detectors belonging to this group, for Ar, Ni, Xe, Ta and, for part of the rings, for Au ions. In Fig. 3 are plotted versus $100/Z$ the average values $-\langle b(Z)\rangle$ concerning the groups III, VI and IX. The Ni ion PHD was measured during each experiment, in two circumstances: with and without gas in the IC. The values were found to be very stable. All the data are well fitted by an equation of type (10), which provides the coefficients p_1 and p_2. There are 9 sets of coefficients i.e. a unique set for one of the 9 found groups instead of an individual set for each of the 180 Si detectors. As no very heavy fragments hit ring 8 and 9 during the INDRA experiments the Ta and Au data from groups VIII and IX, which were found to differ from the log dependence (see Fig. 3), have not been taken into account to calculate p_1 and p_2 values. The last two columns of Table 3 give the values of the two parameters of eq. (10) found in this work. For comparaison are also shown the values obtained in the original work [4] concerning Si-surface barrier detectors and in ref [1] for recent ion-implanted Si detectors PHD data. In the three works the $a(Z)$ dependence (9) has been considered. The empirical character of the parametrization used reveals itself through the disparate values of parameters p_1, p_2. The coefficients displayed in Table 3 are then used to calculate the PHD values of our elastic scattering data, to be compared with the average experimental value $\langle PHD\rangle \pm \sigma$ of each group. This comparison is shown in Fig. 4 for the $\langle PHD\rangle$ of Ni,

12

Xe and Ta. The Moulton recipe, applied to groups of detectors, reproduces the mean experimental values mostly within 10% precision when PHD larger than 30 MeV are measured. For smaller PHD values, relative errors can reach around 30%; in this case the major part of errors come from the precision of 2% (see 3.1) in the determination of E_{alpha} in PHD calculations. The absolute PHD values can be compared to those obtained with surface barrier detectors with low resistivity (around 1KΩcm) especially devoted to the detection of heavy fragments or residues. Low PHDs observed for detector groups I, III, V and VII are found quite close to energy extrapolated values from ref. [4]: they are respectively around 5-10, 50-100 and 100-150 MeV for Ni, Xe and Ta in studied energy ranges. This may be surprising in view of the low electric field strength of the INDRA detectors and can be understood with the arguments presented in section 3.1 and in [2]. For ions passing through the silicon layer, the PHD data are rather well estimated by considering the energy deposited in the Si detectors.

4.3 PHD corrected energies for heavy fragments

The last test is to compare the energy values determined by means of the whole presented procedure, including PHD corrections done for groups of detectors, with the true energy values of the elastic scattering data for: Ar, Ni, Xe, Ta and Au ions, calculated as mentioned at the end of section 3. An iterative routine is used, starting with the initially measured value of the energy as furnished by the classical procedure for LCPs described in section 3. This value is incremented at each step with the ΔE quantity resulting from equation (8), up to a relative variation of $5 \cdot 10^{-3}$. The last value of ΔE is adopted as the actual PHD value, described in this section. Fig. 5 shows the relative deviation of the determined values of the energy of the Ni and Ta ions with respect to the true energy values for every module. It is -0.12% (1.6%) on average for Ni (Ta) and it never exceeds 5-6 %.

5 Comparison to calculations for PHD

In this section we shall present comparisons between some experimental data and calculations which take into account qualitative and some quantitative physical arguments in calculating PHDs. For this comparison we have only selected PHD values from groups I, III, V and VII, which constitute the most homogeneous set of data.
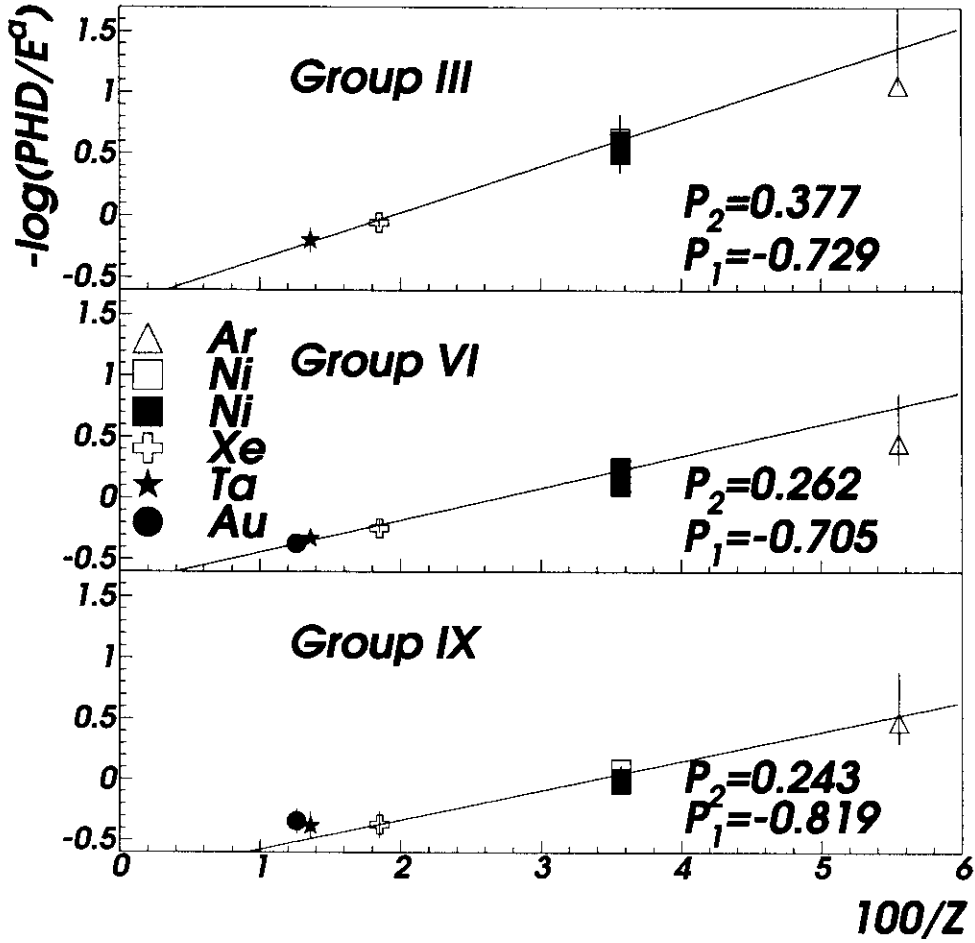
Fig. 3. Dependence of -b(Z) versus 100/Z for groups III, VI and IX (see text for explanations). Open symbols refer to the first experimental campaign (1993) and full symbols refer to the second experimental campaign (1994) performed with INDRA.

5.1 A simple recombination model

As mentioned in subsection 4.1, the recombination process has an important contribution to the PHD value when high carrier concentrations are produced by strongly ionizing fragments at energy high enough to neglect (within 5 – 11 % [16] for our data) the role of the nuclear stopping. The plasma formed in the wake of an ionizing particle slowing down in a silicon detector disappears through extraction of carriers by the electric field in the detector (with a time constant t_p) or by recombination of electrons and holes (of time constant t_r) [6,17,18]. The starting point is to express the ratio of the recombination defect Δ_r to ion energy E_0 as: $\frac{\Delta_r}{E_0} \approx \frac{t_p}{t_r}$, if $t_p \ll t_r$ [18]. The time recombination
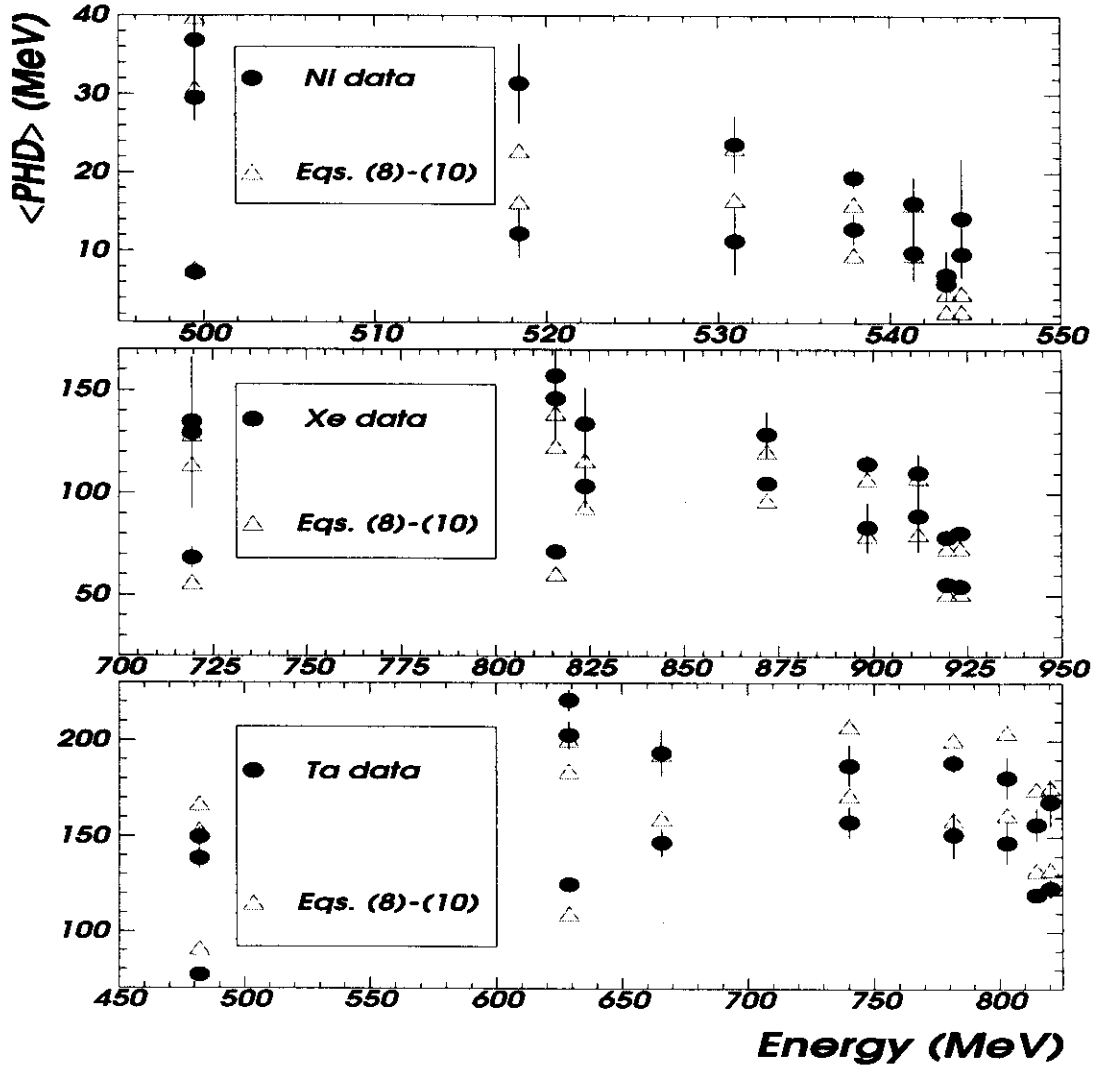
14

Fig. 4. Comparison of the predictions of eqs. (8)-(10) (triangles) with the experimental average pulse height defect (circles) in each group of detectors as a function of the energy deposited by Ni, Xe and Ta ions. Bars represent σ of PHD distributions within a group. The energy is different for the two rings belonging to the same group (see Tables 2 and 3).

constant t_r is inversely proportional to the carrier concentration, i.e. to the energy loss of the incident particle. The opportunity to use a large set of data presented above (detector characteristics and different ions with rather long ranges (40 – 100 μm)) led us to try to quantify the recombination process by taking into consideration the exact variation of the specific electronic stopping power along the particle track. In spite of the diffusion, before the extraction of the plasma by the electric field, a very high carrier concentration is maintained in the proximity of the particle path [17]. Its value remains proportional to the initial number of carriers per unit length given by the specific stopping power. Moreover, the transverse outflow of the carriers is somehow inhibited
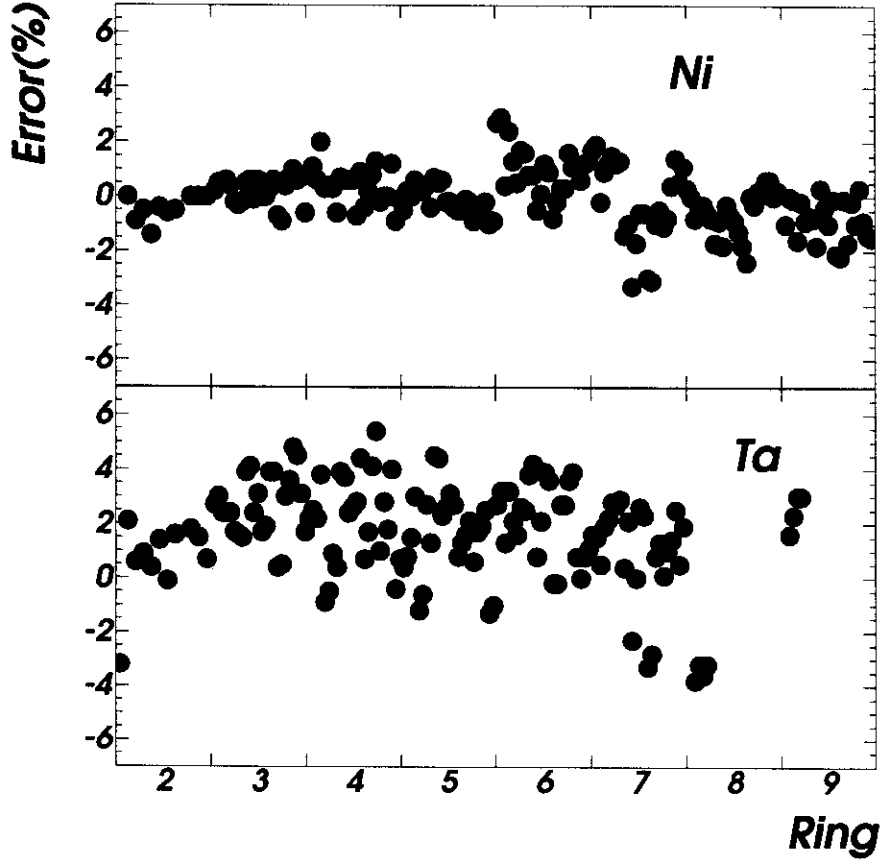
15

Fig. 5. Deviations (in %) of the determined energy values from the true energy values for Ni and Ta ions.

by space charge effects. In so far, the radial diffusion is not considered. The rate equation for the electron concentration $n_e(x,t)$ is: $-\frac{dn_e(x,t)}{dt} = \lambda_p n_e(x,t) + \lambda_r n_e(x,t)n_h(x,t)$, where $n_h(x,t)$ refers to the holes. If $n_h(x,t) = n_e(x,t) = n(x,t)$, the equation of the carrier concentration variation with time reads:

$$-\frac{dn(x,t)}{dt} = \lambda_p n(x,t) + \lambda_r n^2(x,t) \tag{12}$$

where the two terms in the right hand side are related to the signal and to PHD, respectively, with the solution:

$$n(x,t) = \frac{\lambda_p n_0(x)}{(\lambda_p + \lambda_r n_0(x))e^{\lambda_p t} - \lambda_r n_0(x)} \tag{13}$$

16

Here, $n(x,t)$ is the carrier concentration at coordinate x along the trajectory and $n_0(x)$ is its initial value: $n_0(x) = \frac{1}{\epsilon \pi r_0^2}|\frac{dE}{dx}|$, expressed as a function of the stopping power $S = |\frac{dE}{dx}|$, the ionisation potential $\epsilon = 3.6$ eV and the plasma wake transverse area πr_0^2 ($r_0 \approx 1\mu m$ [17], but in the following it is not numerically used); λ_p (the reciprocal of the plasma life time t_p) and $\lambda_r n_0(x)$ (the reciprocal of the recombination time t_r) are related to the two processes: plasma extraction by the electric field and recombination, respectively. The rate of the infinitesimal PHD is related to the square term in equation (12): $\frac{d^2 PHD(x,t)}{dxdt} = \epsilon \pi r_0^2 \lambda_r n^2(x,t)$. The integration over time and over the range $R(E_0)$, or by changing the variable, over the energy, leads to the value of the total PHD:

$$PHD(E_0) = E_0 - \int\limits_{0}^{E_0} \frac{\lambda_p \epsilon \pi r_0^2}{\lambda_r S(E)} \ln\left(1 + \frac{\lambda_r S(E)}{\lambda_p \epsilon \pi r_0^2}\right) dE \qquad (14)$$

where E_0 is the initial energy of the particle and $S(E) = |\frac{dE}{dx}|$ is the stopping power at the energy E. The electric field strength F has a linear dependence on the depth x (eq. (1)), while the electronic stopping power varies much more steeply with x. This is why $\lambda_p \propto F$ [17] may be considered as being practically constant face to the stopping power variation. Let us consider the approximation $S(E) = C \cdot AZ^2/E$ of the Bethe-Bloch formula of the stopping power and put $a = \frac{\lambda_r C}{\lambda_p \epsilon \pi r_0^2}$, where A and Z are the mass and atomic number respectively, C is a constant and a a parameter. The equation (14) may be now analytically integrated over the energy to get a one parameter formula for the PHD:

$$PHD(E_0) = \frac{1}{2}E_0 \left(1 - \frac{1}{a\frac{AZ^2}{E_0}} \ln\left|1 + a\frac{AZ^2}{E_0}\right| + a\frac{AZ^2}{E_0} \ln\left|1 + \frac{1}{a\frac{AZ^2}{E_0}}\right|\right). (15)$$

The ratio $\frac{PHD(E_0)}{E_0}$ vs $\frac{AZ^2}{E_0}$ is plotted in Fig. 6 for the groups I, III, V and VII of detectors, i.e. the groups of lowest experimental PHD values. The plotted curves correspond to equation (15) with values of the parameter a obtained by minimizing the χ^2 for each detector group. The parameter a is connected to the ratio $\frac{t_p}{t_r n_0(x)}$: the plasma life time t_p is proportional to the reciprocal of the electric field strength [17] and the product $t_r n_0(x)$, to the minority carrier life-time $t_0=52\rho^{0.6}$ [18]; t_0 is in μs and ρ in Ωcm. Consequently, the different values of the parameter a may be related to the different characteristics of the silicon detector groups (electric field F and resistivity ρ). The top box in Fig. 6 shows that the a values vary linearly with $(F_{min}\rho^{0.6})^{-1}$ as expected. For simplicity, we took for the electric field strength the values of F_{min} from Table 1, which is not unreasonable because the involved heavy ions are stopped in the first third of the detector thickness. The t_p/t_r ratio for ions at low energies

Table 4

Comparaison of t_p/t_r ratio in a low resistivity surface barrier detector [6] estimated as follows: a) ref [6] based on ref [17,18]; b) ref [6]; c) present work.

Ion	Energy [MeV]	$t_p/t_r^{a)}$	$t_p/t_r^{b)}$	$\langle t_p/t_r \rangle^{c)}$
^{79}Br	38	$0.91 \cdot 10^{-1}$	$2.5 \cdot 10^{-2}$	$3.7 \cdot 10^{-1}$
^{127}I	115	$2.7 \cdot 10^{-1}$	$6.6 \cdot 10^{-2}$	$4.5 \cdot 10^{-1}$

was determined in [6] from PHD data obtained in a low resistivity surface barrier silicon detector. The calculations were done with two assumptions: supposing the simple dependence $t_0 \propto \rho^{0.6}$ [17,18] or a more complicated one $t_0 \propto E_d\rho^{0.32}/(A^{1.2}Z^{0.46})$ [6], where E_d is the energy deposited in the detector by the ion. For the same case we have also estimated the average t_p/t_r ratio by means of the linear dependence shown in the upper box of Fig. 6. For comparaison the values are synthetized in Table 4. As they rely on the same expression of $t_0 \propto \rho^{0.6}$, the results of our estimation and those based on [17,18] are of the same order of magnitude.

The one parameter PHD formula of equation (15) globally reproduces the experimental data, as shown in Fig. 7. This means that the recombination process, described as above, reasonably accounts for the measured experimental values, and is therefore the dominant process creating PHD in the conditions (ion energy, negligible entrance window, charge encoding) used in the present experiment. Table 4 suggests that the applicability of the present approach can thus be enlarged to low resistivity silicon detectors provided that the window and nuclear contributions to the total PHD are negligible or, if not, that they have been previously subtracted [16] from the experimental PHD.

5.2 Comparison with other PHD calculations

Two other calculations, taken from literature, are compared to the experimental PHD data for groups I, III, V and VII. Kaufman calculation [5] was in principle dedicated to PHD for low energy heavy ions (below 100 MeV total energy). PHD is then expressed as a sum of a nuclear stopping defect plus an empirical term designed to fit the data. This empirical term contains a parameter A related to the silicon resistivity. To fit the ^{129}Xe PHD data the necessary values of A (100, 130, 190, 130) increase with the $F\rho$ products. But this approach completely fails in describing the PHD data for ^{58}Ni and ^{181}Ta (see Fig. 7).

Ogihara calculation [6] gives absolute values of PHD as a function of the incident energy E_0, ion mass and atomic number, resistivity, effective electric field strength (that we considered at the middle of the ion range R) and stopping power (for which we took the mean value given by the ratio E_0/R).
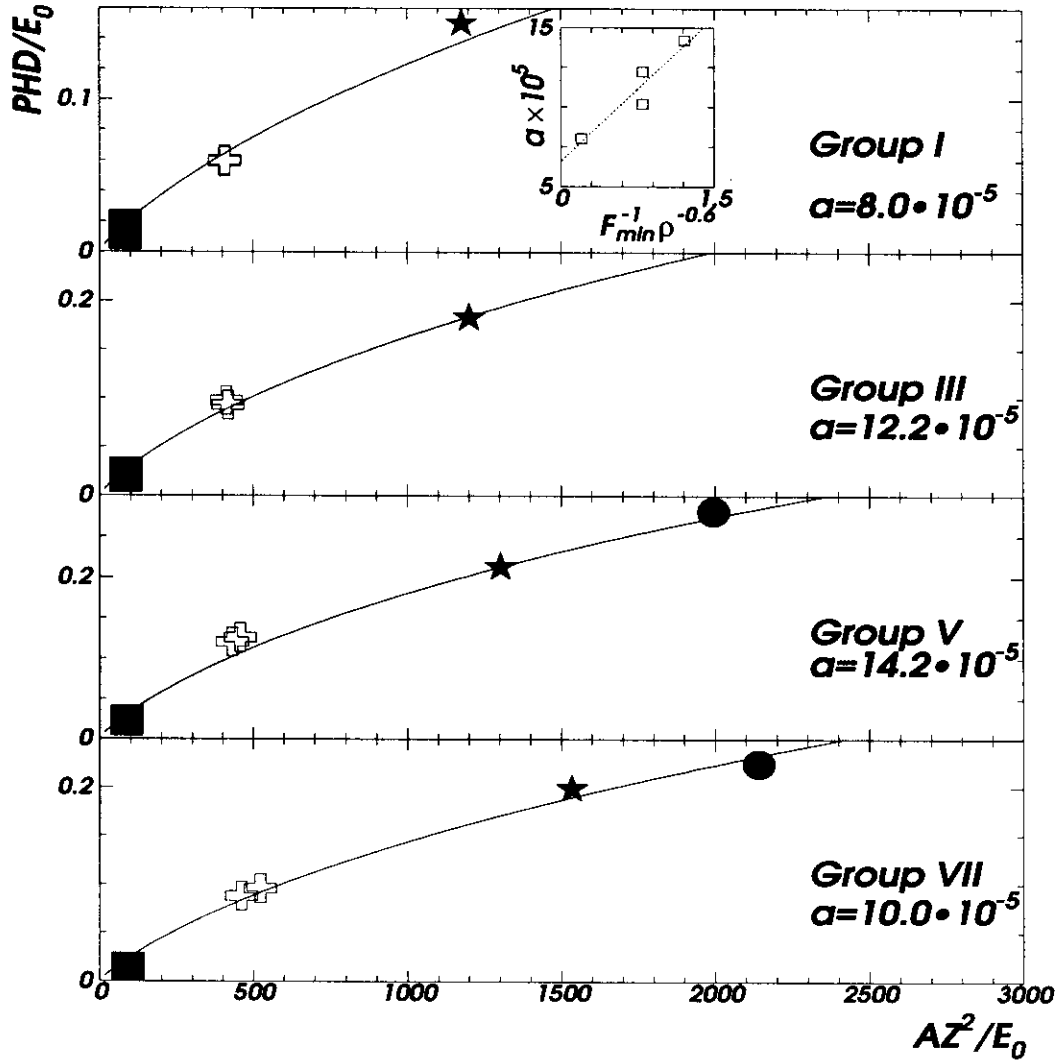
Fig. 6. The ratio $\frac{PHD}{E_0}$ vs $\frac{AZ^2}{E_0}$ for: ^{58}Ni (squares), ^{129}Xe (crosses), ^{181}Ta (stars) and ^{197}Au (circles). The data concern groups I, III, V and VII. The curves were obtained by fitting with formula (15) developed in this work. The fit parameter a is plotted vs $(F_{min}\rho^{0.6})^{-1}$ in the upper box (see text).

The formula in ref. [6] was obtained by fitting low energy PHD data in Si-surface barrier detectors, window defect included. In spite of the fact that in planar silicon detectors the windows are at least one order of magnitude thinner, the predictions of this recipe underestimate our data, especially for the heavier ions (see Fig. 7). They follow however the general trend connected to the effective electric field and silicon resistivity dependence of the PHD.
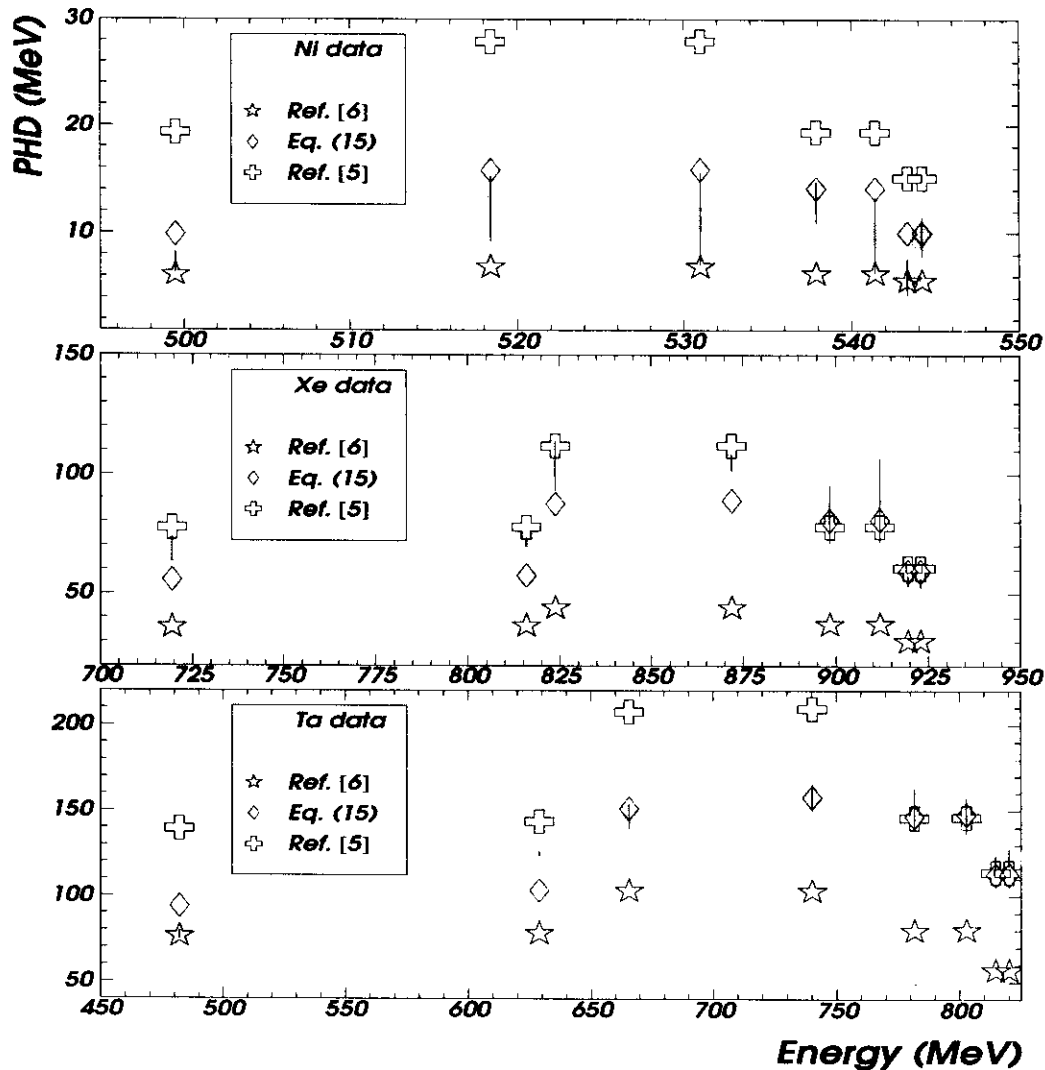
19

Fig. 7. Same as Fig. 4 but data (groups I, III, V, VII) are now compared to the three parametrizations described in section 5.

6 Conclusions

A reliable calibration procedure for the 180 silicon detectors (300 μm thick) of INDRA was developed. The detectors have high resistivity ($\approx$10 KΩcm) and are placed in such a way that the particles enter the detector by the low electric field side. For heavy fragments, an absolute energy calibration of the silicon detectors is carried out by measuring the elastic scattering of low energy (6 – 10 AMeV) heavy ion beams on a gold target. The beams selected are Ar, Ni, Xe, and Ta. All the silicon detectors are calibrated simultaneously. For part of the detectors, the recoil Au elastic scattering data were available. These measurements showed that for ions which stop in the silicon detectors, there is no PHD if their atomic number Z is lower than 10. The PHD remains low

20

if Z is lower than 20, and becomes more and more important for increasing values of Z: quantitatively PHD represent 0–2% of the energy for 8 AMeV Ar ions, 1–9% for 9 AMeV Ni ions, 5–9% (7–25%) for 7 (5.6) AMeV Xe ions and 12–21% (19–36%) for 4.4 (3.6) AMeV Ta ions. The PHD depends on the individual silicon wafer. The PHD data were fitted with a simple power law as used for surface barrier detectors [4]. The procedure ensures a precision better than 2 % on average for the energy response of all heavy ions. For heavy ions which punch through the silicon detectors PHD data are compatible with this parametrization.

The available set of data allowed to test a new and simple recombination model without radial diffusion to account for the PHD of an ionizing particle. A simple one parameter relation between PHD and mass, charge and energy of the particle is obtained. The fit parameter is directly connected to the ratio of the plasma life-time to the recombination time, i.e. to detector characteristics (electric field strength and resistivity).

Finally, two other available calculations are confronted to our experimental PHD data. The formalism of Kaufman and coworkers [5] developed for very low energies completely fails in predicting PHD for ions in the energy range 3.5–9 AMeV. The formula of Ogihara et al [6], which takes into account the electric field strength and resistivity of the detectors, follows the general trend of the data but the precision of its predictions is not sufficient for a calibration purpose.

References

[1] G. Pasquali, G. Casini, M. Bini, S. Calamai, A. Olmi, G. Poggi, A. A. Stefanini, F. Saint-Laurent, J.C. Steckmeyer, *Nucl. Instr. and Meth. A 405 (1998) 39.*

[2] J. Pouthas et al, *Nucl. Instr. and Meth. A 357 (1995) 418.*

[3] J. Pouthas et al, *Nucl. Instr. and Meth. A 369 (1996) 222.*

[4] J.B. Moulton, J.E. Stephenson, R.P Schmitt and G.J. Wozniak, *Nucl. Instr. and Meth. 157 (1978) 325.*

[5] S.B. Kaufman, E.P. Steinberg, B.D. Wilkins, J. Unik, A. J. Gorski, *Nucl. Instr. and Meth. 115 (1974) 47.*

[6] M. Ogihara, Y. Nagashima, G. Galster and T. Mikumo, *Nucl. Instr. and Meth. A 251 (1986) 313.*

[7] *Eurisys Mesures (formerly Intertechnique), 1 Parc des Tanneries, 67380 Lingolsheim, France.*

[8] J. Kemmer, *Nucl. Instr. and Meth. A 226 (1984) 89.*

[9] K. Falk, P.A. Tove and M. Madakbas, *Nucl. Instr. and Meth. 34 (1965) 157.*

[10] N. Copinet, *thèse docteur ingénieur, Caen Univ. (1993).*

[11] F. Hubert, R. Bimbot and H. Gauvin, Range and stopping-power tables for 2.5-500 MeV/nucleon heavy ions in solids, *At. Data and Nucl. Data Tables 46 (1990) 1.*

[12] R. Bimbot, *private communication*

[13] P. Dreier, *Nucl. Instr. and Meth. A 288 (1990) 272.*

[14] F.Z. Henari, E.C. Finch and C.F.G. Delaney, *Nucl. Instr. and Meth. A 288 (1990) 439.*

[15] H. A. Rijken, Ph. D. thesis, Eindhoven Tech. Univ. (1993)

[16] B.D. Wilkins, M.J. Fluss. S.B. Kaufman, C.E Gross and E.P. Steinberg, *Nucl. Instr. and Meth. 92 (1971) 381.*

[17] W. Seibt, K.E. Sundstrom and P.A. Tove, *Nucl. Instr. and Meth. 113 (1973) 317 and references therein*

[18] E.C. Finch, M. Asghar and M. Forte, *Nucl. Instr. and Meth. 163 (1979) 467.*